

Cumulative Treatment Effect Testing under Continuous Time Reinforcement Learning

Jiuchen Zhang¹ and Annie Qu¹

¹*Department of Statistics, University of California, Irvine*

Abstract

Understanding the impact of treatment effect over time is a fundamental aspect of many scientific and medical studies. In this paper, we introduce a novel approach under a continuous-time reinforcement learning framework for testing a treatment effect. Specifically, our method provides an effective test on carryover effects of treatment over time utilizing the average treatment effect (ATE). The average treatment effect is defined as difference of value functions over an infinite horizon, which accounts for cumulative treatment effects, both immediate and carryover. The proposed method outperforms existing testing procedures such as discrete time reinforcement learning strategies in multi-resolution observation settings where observation times can be irregular. Another advantage of the proposed method is that it can capture treatment effects of a shorter duration and provide greater accuracy compared to discrete-time approximations, through the use of continuous-time estimation for the value function. We establish the asymptotic normality of the proposed test statistics and apply it to OhioT1DM diabetes data to evaluate the cumulative treatment effects of bolus insulin on patients' glucose levels.

1 Introduction

Understanding how treatment effects evolve over time is crucial for advancing personalized medicine and improving patient outcomes. With the increasing adoption of mobile health technologies, wearable devices can generate a wealth of longitudinal data, tracking individuals' physical activities and health statuses in real time. These advancements enable the delivery of non-invasive interventions which can be adapted dynamically to patients' needs. However, analyzing such data could be challenging, particularly due to the sequential nature of treatments and their potential influence to future outcomes—a phenomenon known as the carryover effect.

In particular, the challenge in analyzing treatment effects in mobile health studies lies in the complexity of longitudinal data. Treatments are administered as either discrete or continuous interventions, and often have both immediate and cumulative effects on outcomes. Moreover, wearable device data introduce additional layers of complexity, including high-frequency multivariate observations, multi-resolution data, and irregular time intervals.

Existing methods for analyzing dynamic treatment effects in longitudinal settings have made significant progress but face limitations for irregular and heterogeneous mobile health data (Zhang et al., 2024). Causal inference methods for continuous-time interventions, such as Zhang et al. (2011), focus on estimating average treatment effects (ATE) at specific time points. These methods typically assume no carryover effects beyond the observation window and require balanced time intervals for data collection. These methods are effective in controlled experiments, they are incapable of capturing the cumulative effects of treatments over time, which are critical in mobile health studies as interventions are administered dynamically based on real-time data.

To address temporal causal effects, Bojinov and Shephard (2019) introduced the concept of p -lag treatment effects, which examines average treatment impacts over discrete time series experiments. While this approach is well-suited for experiments with fixed-time intervals, it does not accommodate irregular observations or continuous-time processes. Similarly,

research in reinforcement learning, such as Shi et al. (2022a) and Shi et al. (2022b), provide insights on long-term treatment effects using value functions and off-policy evaluation. However, these type of approaches are applied to discrete-time settings, and assume regular observation intervals, which might not be feasible for densely observed and irregular data collected from wearable devices.

Recent methods also addressed challenges associated with treatment changes over time. Schomaker et al. (2024) introduced causal inference techniques tailored for continuous, multiple time-point interventions, particularly relevant in pharmacology with dynamic treatments. Their approach effectively models these dynamic changes. However, it assumes regularly spaced observations and does not explicitly account for cumulative carryover effects. Similarly, Turkel (2019) investigated machine learning-based approaches for continuous treatments, utilizing advanced computational methods to estimate causal effects in complex treatment settings. However, these methods rely on large datasets and are not suited in handling noisy and sparse mobile health data.

To address these challenges, we propose a continuous-time reinforcement learning framework designed to test cumulative treatment effects while accounting for both immediate and carryover impacts. In contrast to existing methods, our approach leverages multi-resolution wearable device data to capture complex temporal dynamics in the state process. By estimating the infinitesimal generator of the underlying continuous-time system, our approach accommodates irregularly spaced observations and provides accurate trajectory estimates for state-process dynamics. This framework allows for robust testing of treatment effects in continuous time, even in the presence of high-frequency and noisy data, thus offering a significant improvement over existing methods.

In addition, the proposed method offers several key advantages and addresses the limitations of existing approaches. First, by separating the estimation of the infinitesimal generator and the value function, we effectively integrate multi-resolution data, enabling the incorporation of diverse observations from wearable devices. This separation not only enhances the robustness of our model but also improves the accuracy of value function estimations by

capturing the refined trajectories in the state process.

Second, our framework is highly flexible in accommodating various stochastic process structures. This flexibility and robustness make it particularly well-suited for high-frequency, irregularly spaced data that are common in wearable device applications. By explicitly modeling accumulative carryover effects over extended periods and utilizing a continuous-time formulation, our method enables more accurate assessment of treatment efficacy. These capabilities support the evaluation of treatment effects, which is a critical step toward informing the design and implementation of adaptive interventions, such as tailoring specific recommendations or managing chronic conditions in real time. Beyond mobile health, the framework can be extended to other domains involving continuous-time processes, such as financial modeling (Sundaresan, 2000) and climate studies (Haurie, 2003), where testing cumulative effects is important.

The remainder of this paper is organized as follows: Section 2 provides an overview of related work and introduces the theoretical foundation of the proposed framework. Section 3 outlines the methodological development and provides implementation details. In Section 4, we establish the theoretical guarantees for the testing procedure, including the asymptotic normality of the proposed test statistics. Section 5 demonstrates the effectiveness of our approach through simulation studies. Section 6 presents an application to real-world mobile health data, and Section 7 concludes with a discussion of our method and directions for future research.

2 Background and Notations

This section provides background and notations for a continuous-time reinforcement learning framework and outlines a potential outcome model under this framework.

We denote an infinite time horizon by $[0, \infty)$. For participant i , let $\bar{a}_{it} = \{a_{is} : 0 \leq s < t, a_{is} \in \mathcal{A}\}$ represent an arbitrary treatment history up to time t , where \mathcal{A} denotes the set of possible treatment options. The counterfactual state at time t , given the treatment

history \bar{a}_{it} , is denoted by $S_{it}^*(\bar{a}_{it})$, providing the hypothetical state that would have occurred under different treatment choices. The state space is a compact set $\mathcal{S} \subseteq \mathbb{R}^d$, representing d -dimensional time-varying covariates. Similarly, the counterfactual outcome at time t , denoted by $Y_{it}^*(\bar{a}_{it})$, refers to the potential outcome that would have been observed under specific treatment decisions.

Additionally, the observed state $(\mathbf{S}_{it})_{t \geq 0}$ maps from $[0, \infty)$ to the state space \mathcal{S} , and provides the trajectory of participant i 's state over time. Finally, the observed treatment history is denoted as $(\bar{A}_{it})_{t \geq 0}$ through mapping to \mathcal{A} to show the sequence of actions chosen by participant i . In this paper, the action space is set as binary, with $\mathcal{A} = \{0, 1\}$, which represents a binary decision: either take or not take treatment. The observed outcome for participant i is denoted as $(Y_{it})_{t \geq 0}$ to provide the observed immediate reward at time t .

The deterministic policy function, $\pi(a|\mathbf{s})$, is a time-homogeneous function which maps the state \mathbf{s} to the set of available actions a . Additionally, we assume that the state function $(\mathbf{S}_{it})_{t \geq 0}$, under the policy $\pi(a|\mathbf{s})$, is a Feller-Dynkin process (Rogers and Williams, 2000) with a transition semigroup $(P_t^\pi)_{t \geq 0}$ and infinitesimal generator \mathcal{L} . We use $S_{it}^*(\pi)$ and $Y_{it}^*(\pi)$ to denote the associated potential state and outcome that would occur at time t if the agent follows π .

The value function, $V^\pi : \mathcal{S} \rightarrow \mathbb{R}$, represents the expected accumulated reward when following the policy π from a given state \mathbf{s} . It is defined as:

$$V^\pi(\mathbf{s}) \triangleq \int_0^\infty \gamma^t \mathbb{E}[Y_{it}^*(\pi) \mid S_{i0} = \mathbf{s}] dt,$$

where S_{i0} is the initial state at time 0 for participant i , and $0 < \gamma < 1$ is a discount factor that balances immediate and future rewards. The value function assesses the effectiveness of the policy π when starting from state \mathbf{s} . Notably, our definition of the value function differs from those commonly found in the literature (Baird, 1994), as $V^\pi(\mathbf{s})$ is defined through potential outcomes rather than observed data.

3 Methodology

In this section, we propose test statistics for treatment effect under a continuous-time reinforcement learning framework. Specifically, we utilize the value functions of two time-invariant policies that assign the same treatment (0 or 1) at each time point to measure the accumulative treatment effects, both immediate and carryover. In addition, the corresponding identifiability of the average treatment effect (ATE) and the testing procedure is established.

3.1 Identifiability of average treatment effect (ATE)

This subsection defines the average treatment effect (ATE) in a continuous-time reinforcement learning framework and outlines that the average treatment effect is identifiable. Our framework generalizes discrete-time results from reinforcement learning and causal inference (such as those of Shi et al. (2022b)) to a continuous-time setting. In doing so, it captures more subtle treatment effects over time, particularly in scenarios with irregular observation intervals or continuously evolving system dynamics.

Consider two baseline policies: one that always applies treatment 0 at every decision time and one that always applies treatment 1. Let $V_0(s)$ and $V_1(s)$ denote the corresponding value functions for an initial state $s \in \mathcal{S}$. Assuming that the reference distribution \mathbb{G} has a bounded density and represents the distribution of the initial state, we define the average treatment effect as the expected difference in value between these two policies:

$$\tau = \int_{\mathcal{S}} \{V_1(s) - V_0(s)\} \mathbb{G}(ds). \quad (1)$$

In words, τ represents the gain in long-term outcome obtained by following the always-1 treatment policy instead of the always-0 policy, averaged over the initial state distribution \mathbb{G} .

Under suitable regularity conditions (see Section 4), the value functions satisfy the fol-

lowing equation for each $a \in \{0, 1\}$:

$$\mathbb{E} [\{Y_{it} + \log \gamma \cdot V_a(S_{it}) + \mathcal{L}V_a(S_{it})\} \varphi(S_{it}, A_{it})] = 0, \quad (2)$$

for any function $\varphi : \mathcal{S} \times \{0, 1\} \rightarrow \mathbb{R}$.

Equation (2) indicates that $V_a(s)$ can be identified directly from the observed data by solving an appropriate estimating equation. Since τ is defined as a functional of V_0 and V_1 , it follows that the average treatment effect is also identifiable under these conditions. The formal assumptions and a detailed identification analysis are provided in Section 4.

To derive the estimating equation, it is necessary to estimate $\mathcal{L}V_a(S_{it})$. We assume that the underlying process S_t evolves according to ordinary differential equation (ODE):

$$dS_t = b(t)dt,$$

where $b(t)$ is the drift coefficient describing the system dynamics.

In this paper, we propose to utilize the derivative of the empirical path for S_{it} as an approximation, which does not impose any assumption on the form of the stochastic process. We use spline functions for numerical derivatives because they provide a smooth approximation of the empirical path, which is particularly useful when dealing with irregularly observed or noisy data. This flexibility allows us to estimate derivatives without imposing restrictive assumptions on the underlying stochastic process.

Specifically, let $\mathcal{S} = \{\chi^\top w : w \in \mathbb{R}^{M \times d}\}$ be a large linear approximation space for S_{it} , where $\chi(\cdot)$ is a vector containing B-spline basis functions $\chi_m(\cdot)$ for $m = 1, \dots, M_s$. Suppose $S_{it} = \chi^\top w_i \in \mathcal{S}$ and the derivative dS_{it}/dt can be estimated as $\nabla \chi^\top w_i$, where $\nabla \chi$ is the derivative of the basis functions χ . However, the observed data X_t includes additive noise, modeled as:

$$X_t = S_t + \epsilon_t,$$

where ϵ_t are i.i.d. centered random variables with zero mean. Using the properties of the

Feller-Dynkin process (Lasota and Mackey, 2013), the infinitesimal generator $\mathcal{L}V_a(S_{it})$ can be expressed as:

$$\mathcal{L}V_a(S_{it}) = \left\langle \frac{dV_a(S_{it})}{dS_{it}}, b(t) \right\rangle, \quad \text{for } a \in \{0, 1\},$$

where $dV_t^\pi(S_t)/dS_t$ is the gradient of the value function with respect to the state S_t , and $\langle \cdot, \cdot \rangle$ denotes the inner product. This relationship allows $\mathcal{L}V_a(S_{it})$ to be estimated by approximating the drift coefficient $b(t)$, in settings where the data are multi-dimensional and observed at discrete, irregular time intervals.

3.2 Test procedure

In practice, solving the estimating equation derived from Theorem 1 can be computationally intensive, particularly in high-dimensional state spaces. In this section, we provide the proposed testing procedure to address these challenges. We fully utilize the identifiability established in Theorem 1 to estimate the value function $V_1(s)$ and $V_0(s)$, and define the accumulative effect with and without treatment respectively. Furthermore, a plug-in estimator of average treatment effect can be established.

Under the previous assumptions, Equation (2) can be rewritten as:

$$\mathbb{E} \left[\left\{ Y_t + \log \gamma \cdot V_a(S_t) - \left\langle \frac{dV_a(S_t)}{dS_t}, b(t) \right\rangle \right\} \varphi(S_t, A_t) \right] = 0. \quad (3)$$

This form highlights how the value function $V_t^\pi(S_t)$ is connected to the system dynamics $b(t)$ and the observed outcomes Y_t . By solving this estimating equation, the value function can be learned, and critical quantities like the average treatment effect (ATE) can be estimated. This estimator is essentially the two-step estimators in Brunel (2008) under the previous settings. The detailed arguments are in the Supplementary materials.

Let $\mathcal{V} = \{\Psi^\top(s)\beta_a : \beta_a \in \mathbb{R}^M\}$ be a large linear approximation space for $V_a(s)$, where $\Psi(\cdot)$ is a vector containing basis functions $\Psi_m(\cdot)$ for $m = 1, \dots, M$ on \mathbb{S} . We define the linear approximation space \mathcal{V} to flexibly capture a wide range of value functions $V_a(s)$. By

using a large basis set $\Psi_m(\cdot)$, we aim to ensure that our approximation space is rich enough to accommodate complex functional relationships between state variables and treatment effects.

Suppose $V_a(s) \in \mathcal{V}$ and set the function $\varphi(s, a)$ in Theorem 1 to $\Psi(s)\mathbb{I}(a = a')$ for $a' = 0, 1$, there exists some $\beta^* = (\beta_0^{*\top}, \beta_1^{*\top})^\top$ such that

$$\mathbb{E} [\{Y_{it} + \log \gamma \cdot \Psi^\top(S_{it})\beta_a^* + \langle \nabla \Psi^\top(S_{it})\beta_a^*, D \rangle\} \Psi(S_{it})\mathbb{I}(A_{it} = a)] = 0, \forall a \in \{0, 1\},$$

where $\mathbb{I}(\cdot)$ denotes the indicator function, $D = w_i^\top \nabla \chi \in \mathbb{R}^d$, $\nabla \chi = (\nabla \chi_1, \dots, \nabla \chi_{M_s}) \in \mathbb{R}^{M_s}$, and $\nabla \Psi(s) = (\nabla \Psi_1(s), \dots, \nabla \Psi_M(s)) \in \mathbb{R}^{d \times M}$. The above equations can be rewritten as $\mathbb{E}(\Sigma_{it}\beta^*) = \mathbb{E}\eta_t$, where Σ_{it} is a block diagonal matrix given with $\Psi(S_{it})\mathbb{I}(A_{it} = 0) \cdot \{-\log \gamma \Psi^\top(S_{it}) - D^\top \nabla \Psi(S_{it})\}$ and $\Psi(S_{it})\mathbb{I}(A_{it} = 1) \cdot \{-\log \gamma \Psi^\top(S_{it}) - D^\top \nabla \Psi(S_{it})\}$, $\eta_{it} = \{\Psi(S_{it})^\top \mathbb{I}(A_{it} = 0) Y_{it}, \Psi(S_{it})^\top \mathbb{I}(A_{it} = 1) Y_{it}\}^\top$.

Let $\widehat{\Sigma} = (nI)^{-1} \sum_{1 \leq i \leq I} \sum_{0 \leq t \leq n} \Sigma_{it}$ and $\widehat{\eta} = (nI)^{-1} \sum_{1 \leq i \leq I} \sum_{0 \leq t \leq n} \eta_{it}$ where I and n denote the number of subjects and the number of observations for each subject i . It follows that $\mathbb{E}\{\widehat{\Sigma}\beta^*\} = \mathbb{E}\{\widehat{\eta}\}$. Consequently, β^* is estimated by

$$\widehat{\beta} = \{\widehat{\beta}_0^\top, \widehat{\beta}_1^\top\}^\top = \widehat{\Sigma}^{-1} \widehat{\eta}.$$

Thus, the average treatment effect can be estimated by the plug-in estimator

$$\widehat{\tau} = \int_s \Psi^\top(s) \{\widehat{\beta}_1 - \widehat{\beta}_0\} \mathbb{G}(ds).$$

One advantage of the proposed estimator is the ability of dealing with multi-resolution data or even irregular observed data (Zhang et al., 2024). When the observation is multi-resolution but not irregular, we can estimate β^* utilizing the time points when the state S_{it} and outcome Y_{it} are all observed, and use the remaining time points for the calculation of numerical derivative D . However, when there is irregularity in the observation, we can still utilize the estimation of empirical path $\chi^\top w_i$ to predict the value of state at time point when

there is only observation of outcome. Specifically, we let $\hat{S}_{it} = \chi^\top \hat{w}_i$ for $t \in \mathbb{T}^Y$, where \mathbb{T}^Y is the index set for the outcome observations Y_{it} . Then let $\hat{\Sigma} = (nI)^{-1} \sum_{1 \leq i \leq I} \sum_{t \in \mathbb{T}^Y} \Sigma_{it}$ and $\hat{\eta} = (nI)^{-1} \sum_{1 \leq i \leq I} \sum_{t \in \mathbb{T}^Y} \eta_{it}$, where n denotes the number of observations of set \mathbb{T}^Y .

Furthermore, we utilize $\hat{\tau}$ to construct our test statistics. Let

$$\mathbf{U} = \left\{ - \int_{s \in \mathbb{S}} \Psi(s)^\top \mathbb{G}(ds), \int_{s \in \mathbb{S}} \Psi(s)^\top \mathbb{G}(ds) \right\}^\top,$$

indicating that $\hat{\tau} = \mathbf{U} \hat{\beta}$. We can show the asymptotic normality of $\sqrt{nI} \{\hat{\tau} - \tau_0\}$ in Section 4. Additionally, the variance of $\sqrt{nI} \hat{\tau}$ can be consistently estimated by

$$\hat{\sigma}^2 = \mathbf{U}^\top \hat{\Sigma}^{-1} \hat{\Omega} \left\{ \hat{\Sigma}^{-1} \right\}^\top \mathbf{U},$$

as n grows to infinity, where $\hat{\Sigma}^{-1} \hat{\Omega} \left\{ \hat{\Sigma}^{-1} \right\}^\top$ is the sandwich estimator for the variance of $\sqrt{nI} \{\hat{\beta} - \beta^*\}$, and that

$$\hat{\Omega} = \frac{1}{nI} \sum_{i=1}^I \sum_{t=0}^{n-1} \left\{ \begin{array}{l} \Psi(S_{it}) (1 - A_{it}) \hat{\varepsilon}_{it,0} \\ \Psi(S_{it}) A_{it} \hat{\varepsilon}_{it,1} \end{array} \right\} \left\{ \begin{array}{l} \Psi(S_{it}) (1 - A_{it}) \hat{\varepsilon}_{it,0} \\ \Psi(S_{it}) A_{it} \hat{\varepsilon}_{it,1} \end{array} \right\}^\top,$$

where $\hat{\varepsilon}_{it,a}$ is the temporal difference error $Y_{it} + \log \gamma \cdot \Psi^\top(S_{it}) \hat{\beta}_a + \langle \nabla \Psi^\top(S_{it}) \hat{\beta}_a, D \rangle$. The sandwich estimator for $\hat{\sigma}^2$ accounts for variability and potential heteroscedasticity in the data, ensuring robust variance estimation. This approach is particularly useful in the presence of multi-resolution or irregularly observed data, where traditional variance estimators may be inadequate. Specifically, the conditional expectation of the temporal difference error given the action $A_{it} = a$ and state S_{it} is zero asymptotically according to Theorem 1. This yields our test statistic $\sqrt{nI} \hat{\tau} / \hat{\sigma}$, which provides a practical tool for evaluating treatment effects in complex, multi-dimensional state spaces. By accommodating multi-resolution and irregularly observed data, the proposed test procedure is well-suited for real-world applications such as personalized medicine.

4 Theory

This section establishes identification of the average treatment effect (ATE) and derives the asymptotic normality of the proposed test statistic. We then formalize the testing procedure that leverages this limit distribution.

4.1 Identification

We first provide sufficient conditions under which the value functions $\{V_a : a \in \{0, 1\}\}$ are identifiable from the observable process. Because the average treatment effect is defined as a functional of V_0 and V_1 via (1), identification of the value functions implies identification of the average treatment effect.

The first two conditions expand the consistency and sequential randomization assumptions in multistage decision-making problems to continuous time.

Assumption 1. (*Consistency Assumption, CA*) $S_{it} = S_{it}^*(\bar{A}_{it})$ and $Y_{it} = Y_{it}^*(\bar{A}_{it})$ for all $t \geq 0$

Assumption 2. (*Continuous-Time Sequential Randomization, CTSR*) There exists a bounded function $\varepsilon(t, \delta) > 0$ with $\int_0^\infty \varepsilon(t, \delta) dt \rightarrow 0$ as $\delta \rightarrow 0$, such that for any $\bar{a}_{it} \in \mathcal{A}, t \in [0, \infty)$, $\delta > 0$

$$\|\mathbb{E} \{Y_{it}^*(\bar{a}_{it}) \mid \bar{A}_{it}, S_{it}\} - \mathbb{E} \{Y_{it}^*(\bar{a}_{it}) \mid \bar{A}_{i,t-\delta}, S_{it}\}\|_1 < \varepsilon(t, \delta)$$

Assumption 2 states that given $\bar{A}_{i,t-\delta}$ and S_{it} , the expectation of $Y_{it}^*(\bar{a}_{it})$ depends only on a short period of treatment assignment between $[t - \delta, t]$. This dependence is upper bounded by this bounded function $\varepsilon(t, \delta)$ whose integral over $t \in [0, \infty)$ tends to zero, as the gap δ goes to zero. The condition $\int_0^\infty \varepsilon(t, \delta) dt \rightarrow 0$ is needed to incorporate longitudinal studies in time range $[0, \infty)$. In discrete time longitudinal studies, this implies sequential randomization assumption that $Y_{i1}^*, \dots, Y_{ik}^* \perp A_{ik} \mid \bar{A}_{i,k-1}, S_{ik}$.

Assumption 3. (*Markov Assumption, MA*) there exists a Feller semigroup $(P)_{t \geq 0}$ such that for any $t' \geq 0$ and $\mathcal{S} \subseteq \mathbb{R}^d$, we have $\Pr \{ S_{i,t+t'}^* (\bar{a}_{it}) \in \mathcal{S} \mid S_{it}^* (\bar{a}_{it}) \} = P_{it'} (\mathcal{S}; a_{it}, S_{it}^* (\bar{a}_{it}))$.

Assumption 4. (*Conditional Mean Independence Assumption, CMIA*) there exists a function r such that for any $t \geq 0$, we have $\mathbb{E} \{ Y_{it}^* (\bar{a}_{it}) \mid S_{it}^* (\bar{a}_{it}) \} = r (a_{it}, S_{it}^* (\bar{a}_{it}))$.

The Assumption 3 and 4 are unique to the reinforcement learning setting. If Assumption 3 holds, Assumption 4 automatically holds when Y_{it} is a deterministic function of S_{it} , A_{it} and $S_{i,t+t'}$ that measures the system's status at time $t + t'$. The latter assumption is commonly made in the reinforcement learning literature, which is a stronger condition than Assumption 4.

Theorem 1. Under the Assumptions to 4, for any $t \geq 0$, $a \in \{0, 1\}$ and any function $\varphi : \mathcal{S} \times \{0, 1\} \rightarrow \mathbb{R}$, we have

$$\mathbb{E} [\{Y_{it} + \log \gamma \cdot V_a(S_{it}) + \mathcal{L}V_a(S_{it})\} \varphi (S_{it}, A_{it})] = 0. \quad (4)$$

Theorem 1 shows that the value function can be estimated directly from the observed data. In particular, one can construct an estimating equation derived from Theorem 1 and learn the value function by solving this equation. Because the average treatment effect (ATE) is defined in terms of the value functions $V_0(s)$ and $V_1(s)$, the identifiability of average treatment effect can be established. This work extends the identification of average treatment effects to continuous-time reinforcement learning settings, accommodating treatment effects that accumulate both immediate effect and carryover effect. Previous studies have mainly addressed discrete time settings, which may fail to address the complexities of continuous processes (Shi et al., 2022b,a). In fact, the discrete-time identification can be seen as a special case of Equation (2), where the infinitesimal generator $\mathcal{L}V_a(S_{it})$ is approximated by

$$\left\langle \frac{V_a(S_{i,t+1}) - V_a(S_{it})}{S_{i,t+1} - S_{it}}, \frac{S_{i,t+1} - S_{it}}{1} \right\rangle,$$

with $\langle \cdot, \cdot \rangle$ representing the inner product.

4.2 Asymptotic properties

To study the asymptotic properties of our procedure, we work under Assumptions 5–9, which tailor standard reinforcement learning conditions to our continuous-time, irregularly sampled setting.

In particular, Assumption 5 allows each subject to be observed on an irregular time grid. Assumption 6 posits exponential β -mixing of the state process, a geometric ergodicity condition in continuous time. This is the continuous-time analogue of the stability conditions commonly used in discrete-time analyses (Bhandari et al., 2018; Shi et al., 2022a). Assumption 7 imposes conditions on the set of basis functions $\Psi(\cdot)$ to ensure that they provide a sufficiently accurate approximation of the value function and the marginalized density ratio. Assumption 8 imposes mild regularity conditions on the action-value temporal-difference errors, specifically requiring their variance to be nondegenerate. Assumption 9 collects regularity requirements that yield normal equations and enable the martingale central limit theorem under irregular sampling.

Theorem 2. *Under Assumption 1 to 9 , we have*

$$\sqrt{nI}(\hat{\tau} - \tau)/\hat{\sigma} \rightarrow^d N(0, 1).$$

In Theorem 2, we demonstrate that the proposed test statistic is asymptotically normal. This result provides the theoretical foundation for hypothesis testing using the standard normal distribution as the reference distribution.

Using the asymptotic normality established in Theorem 2, we propose the following test procedure to evaluate the treatment effect τ . For the null hypothesis $H_0 : \tau \leq 0$ ($H_0 : \tau = 0$) versus the alternative hypothesis $H_a : \tau > 0$ ($H_a : \tau \neq 0$), the test statistic is given by:

$$Z = \sqrt{nI}\hat{\tau}/\hat{\sigma}.$$

The null hypothesis is rejected at a significance level α if:

$$Z > z_\alpha \quad \text{or} \quad |Z| > z_{\alpha/2} \quad \text{for a two-sided test,}$$

where z_α is the upper α -quantile of the standard normal distribution.

The proposed test inherits key statistical properties, including consistency and asymptotic normality, under the assumptions outlined in Theorem 2. These properties ensure that the proposed test maintains correct Type-I error rates and achieves optimal power asymptotically. This procedure is particularly suited for mobile health applications involving multi-resolution and continuous-time data, where traditional methods may struggle to account for temporal dependencies and irregular observation patterns. Therefore, it becomes feasible to detect the treatment effects and their carry-over effects in longitudinal and reinforcement learning frameworks.

5 Numerical Study

In this section, we conduct simulations to investigate the empirical performance of the continuous-time cumulative treatment effect test and compare it with existing methods under different settings. Specifically, we compare the proposed method with three competing methods; namely, the t test (Student, 1908), the double machine learning (DML) test (Chernozhukov et al., 2017), and the SequentiAI Value Evaluation (SAVE) method (Shi et al., 2022b).

The t test is a classical method that is applied to the outcome observations Y_{it} for two groups defined by $A_{it} = 1$ and $A_{it} = 0$. This test, which assumes unequal variances, can be implemented by the Python package `scipy.stats`. The double machine learning method utilizes the state observations to estimate the effect of treatment, which is implemented by the Python package `doubleml`. For the SequentiAI Value Evaluation (SAVE), a method designed for a time-varying setting, we utilize the time point when both state and outcome

are observed and implement with Python module **SAVE**.

We evaluated the effectiveness of the proposed method against the t-test, the double machine learning test, and the the SequentialAI Value Evaluation (SAVE) in two simulation settings. As shown in Figures 1 and 2, the short treatment period resembles bolus insulin therapy, where rapid changes are expected, while the long treatment period mimics basal insulin, where the treatment effect accumulates slowly over time. In both settings, we generated the stochastic process S_t using drift and diffusion functions specified in (5), with an initial value of 0 and a time step of 0.01.

$$\begin{aligned} dS_t &= (-0.2S_t + \delta A_t)dt + \epsilon dW_t \\ Y_t &= S_t \end{aligned} \tag{5}$$

The treatment effect δ was set to 0.3 unless otherwise specified. We sampled t from 0 to 10, with Y_t samples taken every 0.2 and S_t samples taken every 0.1. Noise levels ϵ were varied to reflect different levels of measurement error or variability in physiological responses, which are common in real-world applications such as glucose monitoring or drug efficacy studies.

The null hypothesis is that the new treatment ($A_{it} = 1$) is not better than the old treatment ($A_{it} = 0$), while the alternative hypothesis is that the new treatment is better. The performance of these tests are measured by their power with 50 simulations. We replicated the experiment 200 times in each simulation to calculate the power, considering p-values less than 0.05 as significant.

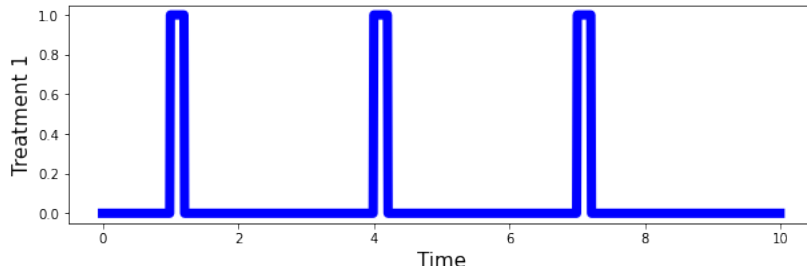


Figure 1: Treatment 1 (short period)

Table 1 compares the power of four methods across two treatment durations—short-term

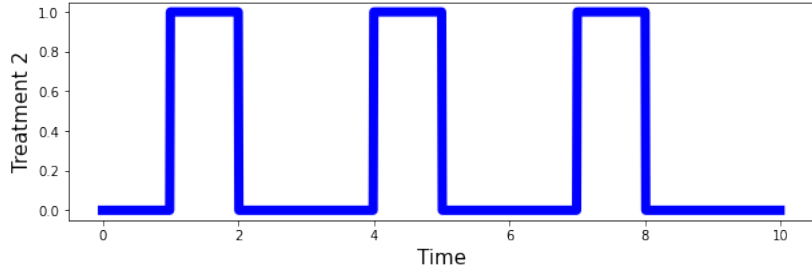


Figure 2: Treatment 2 (long period)

	ϵ	δ	t-test	DML-test	SAVE	Proposed
Treatment 1	0.1	0.3	0.031 (0.012)	0.027 (0.021)	0.221 (0.028)	0.701 (0.031)
		0.0	0.009 (0.007)	0.031 (0.027)	0.049 (0.013)	0.018 (0.008)
	0.3	0.3	0.016 (0.009)	0.025 (0.020)	0.191 (0.029)	0.561 (0.035)
		0.0	0.009 (0.007)	0.031 (0.027)	0.049 (0.013)	0.018 (0.008)
Treatment 2	0.1	0.3	0.002 (0.003)	0.024 (0.019)	0.960 (0.014)	0.988 (0.006)
		0.0	0.038 (0.011)	0.045 (0.030)	0.048 (0.014)	0.033 (0.013)
	0.3	0.3	0.038 (0.013)	0.048 (0.033)	0.758 (0.025)	0.867 (0.029)
		0.0	0.038 (0.011)	0.045 (0.030)	0.048 (0.014)	0.033 (0.013)

Table 1: Test power and Type-I error of competing methods under different treatment assignments and noises ϵ

(Treatment 1) and long-term (Treatment 2) under low and high noise levels. The proposed test is consistently the most powerful, outperforming the Sequential Value Evaluation (SAVE) as well as the *t*-test and double machine learning in every setting, yet it still controls Type-I error conservatively.

The *t*-test's assumption of independent observations prevents it from exploiting temporal dependence, resulting in very low power. The double machine learning, although more flexible through machine-learning adjustments, likewise struggles to capture continuous-time correlations and therefore only marginally surpasses the *t*-test. The Sequential Value Evaluation (SAVE) fares better, particularly for long treatment periods with low noise. However, its power declines when noise increases or the treatment duration shortens, reflecting its limited ability to model fast-changing dynamics.

In contrast, the proposed method maintains strong performance across all scenarios. For instance, under short-term treatment with low noise it attains power close to 0.70 whereas the Sequential Value Evaluation (SAVE) reaches only 0.22 and the classical *t*-test falls be-

low 0.04. Even in the challenging short term, high noise setting it retains power above 0.56, more than twice the SequentiAl Value Evaluation (SAVE) and over twenty times the *t*-test. In long term, high-noise conditions the proposed test still leads with power around 0.87, outpacing the SequentiAl Value Evaluation (SAVE)'s 0.76 and far exceeding the other baselines. These results show that our procedure remains both flexible and practically effective for identifying treatment effects in continuous-time settings, all while maintaining stringent control over false positives.

To evaluate the efficacy of our proposed approach in three complex scenarios, we conducted a comparative analysis against competing methods using a two-state process. Multi-dimensional state spaces are common in real-world applications, such as monitoring multiple physiological markers or financial assets, where interactions between variables must be accurately captured. The stochastic process S_t was generated using the drift and diffusion functions specified in (6), with the same sampling intervals and noise levels as in the univariate case: Y_t samples taken every 0.2, S_t samples taken every 0.1, and noise levels $\epsilon = 0.1$.

Sim1:

$$\begin{aligned} dS_{1,t} &= (-0.1S_{1,t} + \delta A_t)dt + 0.1dW_{1,t} \\ dS_{2,t} &= (-0.3S_{2,t} + 0.5\delta A_t)dt + 0.2dW_{2,t} \\ Y_t &= (S_{1,t} + S_{2,t})/2 \end{aligned} \tag{6}$$

Furthermore, we consider two more complex scenarios: Sim2 (7) and Sim3 (8). In Sim2, the two state processes are positively correlated, reflecting scenarios such as blood pressure and heart rate, where physiological measures are interconnected. Detecting treatment effects in this context is challenging because of the confounding influence of one variable on the other, making it essential for methods to effectively model these relationships to capture the true treatment effect. In Sim3, the treatment effect reverses the trend of the state processes, simulating cases where treatment interventions not only stabilize but actively reverse the progression of a condition (e.g., reversing disease biomarkers). This scenario presents a significant challenge because the treatment effect may act in opposition to the natural progression of the state variables, making it difficult for traditional methods to detect

the full magnitude of the effect.

Sim2:

$$\begin{aligned} dS_{1,t} &= (-0.1S_{1,t} + 0.2S_{2,t} + \delta A_t)dt + 0.1dW_{1,t} \\ dS_{2,t} &= (0.1S_{1,t} - 0.3S_{2,t} + 0.5\delta A_t)dt + 0.2dW_{2,t} \\ Y_t &= (S_{1,t} + S_{2,t})/2 \end{aligned} \quad (7)$$

Sim3:

$$\begin{aligned} dS_{1,t} &= \{(2A_t - 1)(-0.1S_{1,t} + 0.2S_{2,t}) + \delta A_t\}dt + 0.1dW_{1,t} \\ dS_{2,t} &= \{(2A_t - 1)(0.1S_{1,t} - 0.3S_{2,t}) + 0.5\delta A_t\}dt + 0.2dW_{2,t} \\ Y_t &= (S_{1,t} + S_{2,t})/2 \end{aligned} \quad (8)$$

Table 2 demonstrates that the proposed method consistently outperforms the competing methods across all scenarios. In Sim2, where state processes are correlated, the proposed method achieves a power of 0.821, significantly higher than the SequentiAI Value Evaluation (SAVE)’s 0.644. This superior performance likely stems from the proposed method’s ability to model state variables effectively. In Sim3, the proposed method also performs well despite the trend reversal, achieving a power of 0.467, compared to the SequentiAI Value Evaluation (SAVE)’s 0.127 and double machine learning’s 0.193, highlighting its robustness in capturing complex treatment dynamics. The proposed method’s superior performance in multi-dimensional state processes suggests its robustness in capturing complex relationships between state variables. This is likely due to its multi-resolution approach, which allows for flexible modeling of temporal dependencies and interactions between variables, ensuring that even subtle treatment effects are captured. In contrast, methods like the SequentiAI Value Evaluation (SAVE) and double machine learning struggle to adapt to such complexities, leading to lower power in scenarios with correlated states or trend reversals. This robustness is particularly important in real-world applications, such as healthcare, where state variables like heart rate, blood pressure, and glucose levels are often correlated. Accurately detecting treatment effects in such settings is crucial for personalized medicine, where interventions need to account for the complex interplay between multiple physiological factors. Simi-

larly, in finance, where assets are correlated, being able to capture the true effect of market interventions on a portfolio’s performance could provide a critical edge.

	t-test	DML-test	SAVE	Proposed
Sim1	0.000 (0.000)	0.009 (0.016)	0.653 (0.031)	0.990 (0.006)
Sim2	0.000 (0.000)	0.049 (0.032)	0.644 (0.034)	0.821 (0.028)
Sim3	0.000 (0.000)	0.193 (0.053)	0.127 (0.022)	0.467 (0.029)

Table 2: Power of competing methods under different settings

Additional simulations were conducted to further evaluate the proposed method’s performance across different sample sizes and varying levels of treatment effect δ . The complete details—including the specific sample-size grids, the range of δ values examined, and exact performance metrics—are provided in the Supplementary Materials. Overall, these additional results support the consistency and robustness of our proposed estimator, demonstrating reliable statistical performance under diverse sample sizes and effect magnitudes.

6 Real Data Application

In this section, we apply the proposed method to the OhioT1DM dataset (Marling and Bunescu, 2020), a publicly available dataset designed to closely monitor blood glucose level. This dataset provides a comprehensive, multi-resolution set of physiological and self-reported data, making it ideal for evaluating our method on handling continuous time, multi-resolutional data structures in healthcare applications.

The OhioT1DM dataset includes eight weeks of data for twelve patients with type 1 diabetes, divided into two cohorts released in 2018 and 2020. The data includes continuous glucose monitoring (CGM) every 5 minutes, insulin doses (both bolus and basal), and self-reported life events (meals, exercise, sleep, work, stress, and illness) recorded through a custom smartphone app. Additionally, physiological data—such as galvanic skin response (GSR), skin temperature, and acceleration magnitude—is collected, with aggregation frequencies varying by cohort: 1-minute intervals for the 2020 cohort and 5-minute intervals

for the 2018 cohort. Both cohorts consist of individuals on insulin pump therapy.

We focus on the 2020 cohort, which provides high-resolution, 1-minute physiological data. This fine-grained temporal resolution, combined with 5-minute continuous glucose monitoring (CGM) data, introduces a multi-resolution structure.

For analysis, we treat galvanic skin response (GSR), skin temperature, and acceleration magnitude as state processes that may influence blood glucose levels, while continuous glucose monitoring (CGM) serves as the outcome process. We define treatment variables for basal and bolus insulin levels as follows: for basal insulin, $A_{it} = 1$ if the basal insulin level is above the patient’s average basal rate, reflecting a higher-than-usual dose. For bolus insulin, $A_{it} = 1$ when a bolus dose is administered, marking discrete treatments typically used to counteract hyperglycemia or cover carbohydrate intake from meals.

To evaluate each method’s performance, we divide the eight week data collection period into one day intervals to capture day-to-day fluctuations in continuous glucose monitoring (CGM) and physiological measures. We randomly select data from 20 days in each simulation and conduct 100 replications to calculate the power of detecting treatment effects. This simulation setup allows us to assess the robustness of each method through heterogeneous data across subjects.

	t-test	DML-test	Proposed
Basal	0.095 (0.013)	0.147 (0.011)	0.306 (0.032)
Bolus	0.037 (0.014)	0.024 (0.010)	0.647 (0.031)

Table 3: Power of four methods for testing basal and bolus insulin treatment effects in the OhioT1DM dataset.

Table 3 presents the power of four methods—t-test, double machine learning (DML) test, SequentiAl Value Evaluation (SAVE) method, and the proposed method—in detecting basal and bolus insulin treatment effects in the OhioT1DM dataset. The proposed method consistently achieves the highest power across both treatment types.

For basal insulin treatment, all methods show relatively higher power compared to bolus insulin treatment, likely due to the longer, more sustained nature of basal insulin exposure.

This extended longitudinal study allows both immediate and carryover effects to accumulate, making the treatment effect easier to detect.

In contrast, for bolus insulin treatment, which typically involves short term insulin administration, detecting treatment effects is more challenging. Nonetheless, the proposed method demonstrates a notable improvement, at least 28%, over existing methods in this setting, since it accurately captures outcome changes over time using multi-resolution data. These results highlight the proposed method’s enhanced performance in continuous treatment effect estimation. Under the multi-resolution data setting, our model makes valuable contribution for applications such as diabetes management study where treatment responses may vary over time. Our analysis underscores the potential of continuous-time modeling in developing personalized treatment strategies and optimizing continuous monitoring with applications in healthcare.

7 Discussion

In this paper, we propose a novel reinforcement learning-based test procedure for assessing treatment effects in continuous time, utilizing the value function in an infinite horizon to quantify cumulative treatment effects, including both immediate and carryover effects. The proposed test procedure can handle multi-resolution data and accurately estimate changes in the value function over time. Furthermore, the proposed method is effective in scenarios with short treatment periods and weak treatment effects through a newly defined Average Treatment Effect (ATE). Theoretically, we demonstrate the identifiability of the average treatment effect and the asymptotic normality of the proposed test statistic under both null and alternative hypothesis. We showcase the superiority of our method through both simulation and real data applications.

We highlight two potential directions for future research. The first is the development of an online testing framework, which would serve as a valuable tool for real-time monitoring of treatment effects in ongoing clinical trials. The second is an extension of the test proce-

dure to stochastic settings where the state process is governed by a stochastic differential equation rather than an ordinary differential equation. Many real-world processes, especially in mobile health applications, involve intrinsic randomness due to biological variability and environmental influences. Stochastic differential equations explicitly model this randomness through a diffusion term, making them more suitable than ordinary differential equations, which assume deterministic dynamics. This advancement would require further improvements in scalable estimation methods for both drift and diffusion coefficients, particularly in the presence of irregularly observed data arise from mobile health.

References

Baird, L. C. (1994). Reinforcement learning in continuous time: Advantage updating. In *Proceedings of 1994 IEEE International Conference on Neural Networks (ICNN'94)*, v. 4, pp. 2448–2453. IEEE.

Bhandari, J., Russo, D., and Singal, R. (2018). A finite time analysis of temporal difference learning with linear function approximation. In *Conference on learning theory*, pp. 1691–1692. PMLR.

Bojinov, I. and Shephard, N. (2019). Time series experiments and causal estimands: exact randomization tests and trading. *Journal of the American Statistical Association*, 114(528):1665–1682.

Brunel, N. J. (2008). Parameter estimation of ODE’s via nonparametric estimators.

Chernozhukov, V., Chetverikov, D., Demirer, M., Duflo, E., Hansen, C., and Newey, W. (2017). Double/debiased/neyman machine learning of treatment effects. *American Economic Review*, 107(5):261–265.

Haurie, A. (2003). Integrated assessment modeling for global climate change: an infinite horizon optimization viewpoint. *Environmental Modeling & Assessment*, 8:117–132.

Lasota, A. and Mackey, M. C. (2013). *Chaos, fractals, and noise: stochastic aspects of dynamics*, v. 97. Springer Science & Business Media.

Marling, C. and Bunescu, R. (2020). The OhioT1DM dataset for blood glucose level prediction: Update 2020. In *CEUR workshop proceedings*, v. 2675, pp. 71. NIH Public Access.

Rogers, L. C. and Williams, D. (2000). *Diffusions, markov processes, and martingales: Volume 1, foundations*, v. 1. Cambridge university press.

Schomaker, M. et al. (2024). Causal Inference for Continuous Multiple Time Point Interventions. *Statistics in Medicine*, 43:1121–1134.

Shi, C., Wang, X., Luo, S., Zhu, H., Ye, J., and Song, R. (2022a). Dynamic causal effects evaluation in a/b testing with a reinforcement learning framework. *Journal of the American Statistical Association*, pp. 1–13.

Shi, C., Zhang, S., Lu, W., and Song, R. (2022b). Statistical inference of the value function for reinforcement learning in infinite-horizon settings. *Journal of the Royal Statistical Society Series B: Statistical Methodology*, 84(3):765–793.

Student (1908). The probable error of a mean. *Biometrika*, pp. 1–25.

Sundaresan, S. M. (2000). Continuous-time methods in finance: A review and an assessment. *The Journal of Finance*, 55(4):1569–1622.

Turkel, E. (2019). Machine Learning Methods for Continuous Treatments. *CS229 Project Report*, NA:NA.

Zhang, J., Xue, F., Xu, Q., Lee, J., and Qu, A. (2024). Individualized dynamic latent factor model for multi-resolutional data with application to mobile health. *Biometrika*, pp. asae015.

Zhang, M., Joffe, M. M., and Small, D. S. (2011). Causal inference for continuous-time processes when covariates are observed only at discrete times. *Annals of statistics*, 39(1).

8 Appendix

8.1 Additional simulations

Table 4 summarizes the power of the competing methods across different sample sizes under setting Sim1, indicate that both the t-test and DML-test are unsuccessful in detecting the carryover effect, consistent with the one-dimensional state process scenario. Our proposed method continues to outperform the SequentiAl Value Evaluation (SAVE), particularly when the sample size is relatively small (e.g., $n_s = 25$, $n_y = 12$), achieving a power of 0.563 compared to the SequentiAl Value Evaluation (SAVE)'s 0.166. This is due to the method's ability to leverage multi-resolution data, allowing it to effectively capture temporal patterns in the state processes, even when the available data is sparse. the SequentiAl Value Evaluation (SAVE), by contrast, struggles with lower sample sizes as it relies on sequential evaluation, which may not fully capture the dynamic nature of the state processes in such settings.

Sample size	t-test	DML-test	SAVE	Proposed
$n_s = 25, n_y = 12$	0.001 (0.002)	0.020 (0.025)	0.166 (0.027)	0.563 (0.034)
$n_s = 50, n_y = 25$	0.000 (0.000)	0.021 (0.022)	0.599 (0.029)	0.867 (0.022)
$n_s = 100, n_y = 50$	0.000 (0.000)	0.009 (0.016)	0.653 (0.031)	0.990 (0.006)

Table 4: Power of competing methods under different sample sizes

Additionally, we compare the performance of the four methods under varying levels of treatment effect δ in Table 5. The proposed method experiences less power loss compared to the SequentiAl Value Evaluation (SAVE) when handling lower treatment effects. For instance, at $\delta = 0.1$, the proposed method achieves a power of 0.772, compared to the SequentiAl Value Evaluation (SAVE)'s 0.653, indicating a 12% higher power in detecting subtle treatment effects. The proposed method performs particularly well for $\delta = 0.1$ and $\delta = 0.3$, which can be attributed to its ability to effectively model cumulative treatment effects and temporal dependencies within the data. This allows it to detect subtle shifts in the state process that other methods fail to capture. In addition to superior power,

the proposed method effectively controls the Type I error rate, maintaining values close to the 0.05 level under the null hypothesis ($\delta = 0$). This indicates that the method is robust in avoiding false positives while maximizing power. In comparison, other methods fail to maintain reasonably Type I error rates, as seen with the SequentiAl Value Evaluation (SAVE)’s rate of 0.045 and DML’s rate of 0.007.

These findings are particularly relevant in fields such as healthcare, where detecting small but meaningful treatment effects, such as the effect of a new medication or intervention, is critical for patient outcomes. The proposed method’s ability to maintain high power while controlling Type I error underlines its practical utility in these high-stakes scenarios.

δ	t-test	DML-test	SAVE	Proposed
0	0.026 (0.011)	0.007 (0.012)	0.045 (0.015)	0.050 (0.018)
0.1	0.005 (0.004)	0.002 (0.009)	0.653 (0.031)	0.772 (0.027)
0.2	0.000 (0.001)	0.008 (0.013)	0.786 (0.028)	0.941 (0.016)
0.3	0.000 (0.000)	0.009 (0.016)	0.902 (0.021)	0.990 (0.006)

Table 5: Power of competing methods under different treatment effects δ

8.2 Two-step estimator of drift coefficient with noisy data

According to Brunel (2008), the estimation procedure for parameter estimation in ordinary differential equations (ODEs) involves a two-step approach. In the first step, the solution S_t of the ODE and its derivative dS_t/dt are estimated nonparametrically using methods such as smoothing splines, kernel regression, or local polynomial regression. Consistent estimators \hat{S}_t and $d\hat{S}_t/dt$ are constructed such that they converge to the true solution and its derivative under appropriate conditions. The flexibility of nonparametric methods allows for accurate estimation of S_t and dS_t/dt without requiring strong parametric assumptions about the form of the solution. This first step provides a foundation for the subsequent parameter estimation by ensuring that the estimated trajectories and derivatives closely approximate the true dynamics of the system.

In the second step, the parameter θ is estimated by minimizing the discrepancy between

the estimated derivative $d\hat{S}_t/dt$ and the ODE system function $b(t; \theta)$. Specifically, the criterion for optimization is defined as

$$R_{q,n,w}(\theta) = \left\| \frac{d\hat{S}_t}{dt} - b(t; \theta) \right\|_{q,w},$$

where $\|\cdot\|_{q,w}$ represents the weighted L_q -norm. The parameter estimator $\hat{\theta}_n$ is then obtained by solving the optimization problem

$$\hat{\theta}_n = \arg \min_{\theta} R_{q,n,w}(\theta).$$

When smoothing splines are employed in the first step, the solution S_t is represented as $S_{it} = \chi^\top w_i$, where χ denotes the spline basis functions and w_i are the coefficients. Under the assumption that $b(\cdot) \in \mathcal{S}$, the parameter estimate $\hat{\theta}_n$ corresponds directly to the estimated coefficients \hat{w}_i , which determine the fitted spline.

8.3 Proof of Theorem 1

By CA, we may identify the observed state and outcome with their potential outcome counterparts, so that for all times

$$S_t = S_t^*(\bar{A}_t) \quad \text{and} \quad Y_t = Y_t^*(\bar{A}_t).$$

Our goal is to show that

$$\mathbb{E} \left[\left\{ Y_t + \log \gamma V_a(S_t^*) + \mathcal{L} V_a(S_t^*) \right\} \varphi(S_t^*, A_t) \right] = 0,$$

where φ is an arbitrary test function, V_a is the value function, and \mathcal{L} is the infinitesimal generator associated with the Feller process as specified by MA.

To construct the proof, we use a finite-difference approach by comparing the process at time $t + \delta$ with that at time t and then letting the increment δ tend to zero. For any fixed

time t and small $\delta > 0$, define

$$\Delta(\delta) := \gamma^{t+\delta} V_a(S_{t+\delta}^*) + \int_t^{t+\delta} \gamma^u Y_u du - \gamma^t V_a(S_t^*).$$

By the CTSR assumption and the definition of the value function, $\Delta(\delta)/\delta$ tends to 0 as $\delta \rightarrow 0$, since CTSR and the definition of V_a ensure that any finite change over the interval $[t, t + \delta]$ becomes negligible when normalized by δ .

Moreover, the Markov property and the Feller process structure ensure that the finite-difference quotient for the value function term satisfies

$$\frac{\gamma^{t+\delta} V_a(S_{t+\delta}^*) - \gamma^t V_a(S_t^*)}{\delta} \rightarrow \gamma^t \left[\log \gamma V_a(S_t^*) + \mathcal{L}V_a(S_t^*) \right]$$

as $\delta \rightarrow 0$. Similarly, by the mean-value theorem for integrals,

$$\frac{1}{\delta} \int_t^{t+\delta} \gamma^u Y_u du \rightarrow \gamma^t Y_t.$$

Combining these limits yields

$$\gamma^t \left[\log \gamma V_a(S_t^*) + \mathcal{L}V_a(S_t^*) \right] + \gamma^t Y_t = 0.$$

Since $\gamma^t > 0$ for all t , we conclude that

$$Y_t + \log \gamma V_a(S_t^*) + \mathcal{L}V_a(S_t^*) = 0.$$

Multiplying by the test function $\varphi(S_t^*, A_t)$ and taking expectations preserves this equality:

$$\mathbb{E} \left[\left\{ Y_t + \log \gamma V_a(S_t^*) + \mathcal{L}V_a(S_t^*) \right\} \varphi(S_t^*, A_t) \right] = 0.$$

Since the above argument holds at an arbitrary time t and for all $(S, A, Y) \in \mathbb{S} \times \mathcal{A} \times \mathcal{Y}$, and because the recursive construction of the supports for the initial state $S_0 \in \mathbb{S}_0$, actions

$A_t \in \mathcal{A}$, and outcomes $Y_t \in \mathcal{Y}$ is incorporated via CTSR, MA, and CMIA (see, e.g., Shi et al. (2022a,b)), the desired result is established.

8.4 Proof of Theorem 2

Define the marginalized density ratio for the continuous-time setting:

$$\omega_t(a; A, S) := \frac{\mathbb{I}\{A_t = a\} \int_0^\infty e^{-\beta u} p_u^{(a)}(S) du}{\int_0^t \Pr(A_u = A \mid \bar{A}_u, S_u) p_u^{\text{obs}}(S) du}, \quad (9)$$

where $\beta = -\ln \gamma$ is the continuous-time discount rate, $p_u^{(a)}(s)$ denotes the density of the counterfactual state at time u under the “always- a ” policy, $p_u^{\text{obs}}(s)$ is the marginal density of the observed state at time u , and $\Pr(A_u = A \mid \bar{A}_u, S_u)$ is the behavior-policy probability of taking the observed action at time u given the history $\bar{A}_u = \{A_s : 0 \leq s < u\}$ and state S_u .

We also impose the following additional assumptions:

Assumption 5. *Each subject i is observed on an irregular grid $0 = t_{i0} < t_{i1} < \dots < t_{i,N_i} = T_i$, with inter-observation intervals $\Delta t_{ij} := t_{i,j} - t_{i,j-1}$. Either (i) dense sampling (infill): $\max_j \Delta t_{ij} \rightarrow 0$ as $T_i \rightarrow \infty$; or (ii) bounded spacing: $0 < \underline{\Delta} \leq \Delta t_{ij} \leq \bar{\Delta} < \infty$ and $T_i = O(n)$. The I subjects are independent. Write $nI := \sum_{i=1}^I T_i$ for the total follow-up time.*

Assumption 6. *The state process $\{S_{i,t}\}_{t \geq 0}$ is exponentially β -mixing (ergodic).*

Assumption 7. *There exist some coefficient vectors $\boldsymbol{\beta}^* = ((\boldsymbol{\beta}_0^*)^\top, (\boldsymbol{\beta}_1^*)^\top)^\top$ and $\{\boldsymbol{\theta}_{a,t}^*\}_{a,t}$ such that*

$$\sup_{a \in \{0,1\}, s \in \mathcal{S}} |V^a(s) - \Psi(s)^\top \boldsymbol{\beta}_a^*| = o\{(nI)^{-1/4}\},$$

and

$$\sup_{a \in \{0,1\}, s \in \mathcal{S}, t > 0} |\omega_t(a; \bar{A}_t, s) - \Psi(s)^\top \boldsymbol{\theta}_{a,t}^*| = o\{(nI)^{-1/4}\}.$$

Assumption 8. *For some $c_1 > 0$, $\inf_{a,s} \text{Var}\{\varepsilon_{it,a} \mid S_t = s\} \geq c_1$, where $\varepsilon_{it,a} := Y_{it} + \log(\gamma) V_a(S_{it}) + \langle \nabla V_a(S_{it}), D \rangle$ is the temporal-difference error at time t_{it} for action a .*

Assumption 9. $\Psi(s)$ and $\nabla\Psi(s)$ are uniformly bounded. In addition, there exists some $\delta > 0$ such that $\mathbb{E}[\|\Psi(S_t)\mathbb{I}\{A_t = a\}\varepsilon_{t,a}\|^{2+\delta}] < \infty$. Define

$$\Sigma_a(T) := -\frac{1}{T} \int_0^T \mathbb{E} \left[\Psi(S_t) \mathbb{I}\{A_t = a\} \{\nabla\Psi(S_t)^\top b(S_t, a)\}^\top \right] dt,$$

and assume $\Sigma_a(T) \rightarrow \Sigma_a$ as $T \rightarrow \infty$, with each Σ_a nonsingular. Let $\Sigma := \text{diag}(\Sigma_0, \Sigma_1)$.

Part 1:

For notational simplicity, suppose each subject i has n observation intervals (so n observations of (S_{it}, A_{it}, Y_{it}) for $t = 0, 1, \dots, n-1$). Then the total number of observations is nI , and we write sums as $\frac{1}{nI} \sum_{i=1}^I \sum_{t=0}^{n-1}$. We first establish that for each $a \in \{0, 1\}$:

$$\int_{\mathcal{S}} \{\hat{V}_a(s) - V_a(s)\} G(ds) = \frac{1}{nI} \sum_{i=1}^I \sum_{t=0}^{n-1} \omega_t(a; \bar{A}_{it}, S_{it}) \varepsilon_{it,a} + o_p\{(nI)^{-1/2}\},$$

where $\varepsilon_{it,a} := Y_{it} + \log(\gamma) V_a(S_{it}) + \langle \nabla V_a(S_{it}), D \rangle$ is the temporal-difference error at time t_{it} for action a .

The proposed estimator $\hat{\beta} = ((\hat{\beta}_0)^\top, (\hat{\beta}_1)^\top)^\top$ is defined as the solution to the estimating equation $\hat{\Sigma}^{-1} \hat{\eta} = 0$, where

$$\hat{\Sigma} = \frac{1}{nI} \sum_{i=1}^I \sum_{t=0}^{n-1} \Sigma_{it}, \quad \hat{\eta} = \frac{1}{nI} \sum_{i=1}^I \sum_{t=0}^{n-1} \eta_{it}.$$

Here Σ_{it} is a block-diagonal matrix (with blocks corresponding to $a = 0$ and $a = 1$) such that for each $a \in \{0, 1\}$, the $M \times M$ block is $\Psi(S_{it}) \mathbb{I}\{A_{it} = a\} [-\log(\gamma) \Psi(S_{it})^\top - D(t_{it})^\top \nabla\Psi(S_{it})]$. Also, $\eta_{it} = (\Psi(S_{it})^\top \mathbb{I}\{A_{it} = 0\} Y_{it}, \Psi(S_{it})^\top \mathbb{I}\{A_{it} = 1\} Y_{it})^\top$.

We employ a perturbation argument by constructing an auxiliary parameter that adds a small bias in the direction of a chosen function μ^* . For a sequence $\{\delta_n\}$ with $\delta_n = o\{(nI)^{-1/2}\}$, define the auxiliary parameter

$$V^\delta := (1 - \delta_n) \hat{V} + \delta_n (V + \mu^*),$$

where μ^* will be set to either $+\omega_t$ or $-\omega_t$ in the following derivation.

Note that the proposed estimator can be represented as the minimizer of the following least square loss over the sieve space,

$$\arg \min_{\bar{V}} \frac{1}{2nI} \sum_{1 \leq i \leq I} \sum_{0 \leq t \leq n} \left\{ Y_{it} + \log \gamma \cdot \bar{V}_a(S_{it}) + \left\langle \nabla \hat{V}_a(S_{it}), D \right\rangle \right\}^2 \mathbb{I}(A_j = a).$$

Let \mathcal{P}_q denote the projection operator for the above optimization onto the sieve space $\mathbb{V} := \{\Psi(s)^\top \beta : \beta \in \mathbb{R}^M\}$. Under Assumption 7, the sieve approximation error is small: $\|\mathcal{P}_q \mu^* - \mu^*\|_\infty = o\{(nI)^{-1/4}\}$ and $\|\mathcal{P}_q V_a - V_a\|_\infty = o\{(nI)^{-1/4}\}$.

Since $\hat{V} \in \mathbb{V}$, we have

$$\mathcal{P}_q V^\delta = (1 - \delta_n) \hat{V} + \delta_n \mathcal{P}_q(V + \mu^*) = (1 - \delta_n) \hat{V} + \delta_n \{\mathcal{P}_q V + \mathcal{P}_q \mu^*\}.$$

By the definition of \hat{V} as the solution to the estimating equation, we must have

$$\begin{aligned} & \frac{1}{2nI} \sum_{1 \leq i \leq I} \sum_{0 \leq t \leq n} \left\{ Y_{it} + \log \gamma \cdot \hat{V}_a(S_{it}) + \left\langle \nabla \hat{V}_a(S_{it}), D \right\rangle \right\}^2 \mathbb{I}(A_j = a) \\ & \leq \frac{1}{2nI} \sum_{1 \leq i \leq I} \sum_{0 \leq t \leq n} \left\{ Y_{it} + \log \gamma \cdot \mathcal{P}_q V_a^\delta(S_{it}) + \left\langle \nabla \hat{V}_a(S_{it}), D \right\rangle \right\}^2 \mathbb{I}(A_j = a). \end{aligned}$$

Rearranging terms yields the inequality:

$$\begin{aligned} 0 & \geq \frac{1}{nI} \sum_{i,t} \varepsilon_{it,a} \Delta_{it}(\mu^*) \mathbb{I}\{A_{it} = a\} \\ & + \frac{1}{nI} \sum_{i,t} \left[\log \gamma \{\hat{V}_a - V_a\}(S_{it}) + \langle \nabla(\hat{V}_a - V_a)(S_{it}), D \rangle \right] \Delta_{it}(\mu^*) \mathbb{I}\{A_{it} = a\}, \end{aligned} \tag{10}$$

where $\Delta_{it}(\mu^*) := \mathcal{P}_q(V_a + \mu^*)(S_{it}) - \hat{V}_a(S_{it})$.

Since $\|\mathcal{P}_q \mu^* - \mu^*\|_\infty = o\{(nI)^{-1/4}\}$ and $\|\mathcal{P}_q V_a - V_a\|_\infty = o\{(nI)^{-1/4}\}$, we have

$$\Delta_{it}(\mu^*) = \mu^*(S_{it}) + V_a(S_{it}) - \hat{V}_a(S_{it}) + r_{it}, \quad \sup_{i,t} |r_{it}| = o\{(nI)^{-1/4}\}.$$

Additionally, by Assumption 7, we have $\Delta_{it}(\mu^*) = \mu^*(S_{it}) + o\{(nI)^{-1/4}\}$. By a martingale CLT (Assumption 6),

$$\frac{1}{nI} \sum_{i,t} \varepsilon_{it,a} r_{it} \mathbf{1}\{A_{it} = a\} = o_p\{(nI)^{-1/2}\}.$$

Similarly, using $\|\hat{V}_a - V_a\|_\infty = O_p\{(nI)^{-1/4}\}$, the second line of ((10)) is $o_p\{(nI)^{-1/2}\}$ by Cauchy–Schwarz.

Hence, the first term of RHS of (10) is equal to

$$\frac{1}{nI} \sum_{i,t} \varepsilon_{it,a} \mu^* \mathbb{I}\{A_{it} = a\} + o\{(nI)^{-1/2}\}$$

Similarly, we can show that the second term of (10) is $o\{(nI)^{-1/2}\}$. It follows from (10) that

$$0 \geq \frac{1}{nI} \sum_{i,t} \varepsilon_{it,a} \mu^* \mathbb{I}\{A_{it} = a\} + o\{(nI)^{-1/2}\}$$

More precisely, the full expansion implies the balanced identity

$$\frac{1}{nI} \sum_{i,t} \left\{ -\log \gamma \Delta V_a(S_{it}) + \langle \nabla \Delta V_a(S_{it}), D \rangle \right\} \mu^*(S_{it}) \mathbb{I}\{A_{it} = a\} = -\frac{1}{nI} \sum_{i,t} \varepsilon_{it,a} \mu^*(S_{it}) \mathbb{I}\{A_{it} = a\} + o_p\{(nI)^{-1/2}\} \quad (11)$$

Equation (10) is the one-sided version of (11) after the other terms have been shown to be $o_p\{(nI)^{-1/2}\}$.

We next show that

$$\mathbb{E} \left[\left\{ \beta f(S_t) + \langle \nabla f(S_t), D \rangle \right\} \omega_t(a; \bar{A}_t, S_t) \mathbb{I}\{A_t = a\} \right] = \int_{\mathcal{S}} f(s) G(ds), \quad \forall f \in \mathcal{B}, \quad (12)$$

for any bounded measurable f .

Define the discounted occupancy measure of the always- a dynamics,

$$\mathbf{M}^{(a)}(ds) := \int_0^\infty e^{-\beta u} p_u^{(a)}(s) du ds,$$

and the behavior-policy aggregated marginal at evaluation time t ,

$$\mathbb{N}_t^b(ds, a) := \left(\int_0^t b(a \mid \bar{A}_u, S_u) p_u^{\text{obs}}(s) du \right) ds.$$

By (A1), $\mathbb{M}^{(a)}$ is absolutely continuous w.r.t. \mathbb{N}_t^b on $\mathcal{S} \times \{a\}$, and the Radon–Nikodym derivative equals the pathwise quantity in (9):

$$\frac{d\mathbb{M}^{(a)} \otimes \delta_a}{d\mathbb{N}_t^b}(\bar{A}_t, S_t, A_t) = \omega_t(a; \bar{A}_t, S_t) \mathbb{I}\{A_t = a\}.$$

Hence, for any bounded measurable $g : \mathcal{S} \rightarrow \mathbb{R}$,

$$\mathbb{E}_b[g(S_t) \omega_t(a; \bar{A}_t, S_t) \mathbb{I}\{A_t = a\}] = \int_{\mathcal{S}} g(s) \mathbb{M}^{(a)}(ds) = \int_0^\infty e^{-\beta u} \mathbb{E}^{(a)}[g(S_u)] du, \quad (13)$$

where the last equality is Fubini/Tonelli plus the definition of $\mathbb{M}^{(a)}$.

Let $m(u) := \mathbb{E}^{(a)}[f(S_u)]$ for $f \in \mathcal{D}(L)$. By (A3), $m'(u) = \mathbb{E}^{(a)}[Lf(S_u)]$. Integration by parts gives, using (A2),

$$\int_0^\infty e^{-\beta u} \left\{ \beta m(u) + m'(u) \right\} du = \left[e^{-\beta u} m(u) \right]_{u=0}^{u=\infty} = m(0) = \mathbb{E}^{(a)}[f(S_0)] = \int_{\mathcal{S}} f(s) G(ds).$$

Apply (13) with $g = \beta f + Lf$ to obtain

$$\mathbb{E}_b[\{\beta f(S_t) + Lf(S_t)\} \omega_t(a; \bar{A}_t, S_t) \mathbb{I}\{A_t = a\}] = \int_0^\infty e^{-\beta u} \mathbb{E}^{(a)}[\beta f(S_u) + Lf(S_u)] du = \int_{\mathcal{S}} f(s) G(ds),$$

which is (12).

Write $\Delta V_a := \hat{V}_a - V_a$. Set $\mu^* = \omega_t$ in (11) and take expectations of the left-hand side using (12) with $f = \Delta V_a$:

$$\frac{1}{nI} \sum_{i,t} \left\{ \beta \Delta V_a(S_{it}) + \langle \nabla \Delta V_a(S_{it}), D \rangle \right\} \omega_t(a; \bar{A}_{it}, S_{it}) \mathbb{I}\{A_{it} = a\} = \int_{\mathcal{S}} \Delta V_a(s) G(ds) + o_p\{(nI)^{-1/2}\}.$$

Therefore, by (11),

$$\int_{\mathcal{S}} \Delta V_a(s) G(ds) = \frac{1}{nI} \sum_{i=1}^I \sum_{t=0}^{n-1} \omega_t(a; \bar{A}_{it}, S_{it}) \varepsilon_{it,a} + o_p\{(nI)^{-1/2}\}.$$

For completeness, repeating the same argument with $\mu^* = -\omega_t$ gives the reverse one-sided inequality and thus the same stochastic order, which sandwiches the remainder and yields the stated expansion.

Part 2 From Part 1, we have

$$\hat{\tau} - \tau_0 = \frac{1}{nI} \sum_{i=1}^I \sum_{t=0}^{n-1} \omega_t(a; \bar{A}_{it}, S_{it}) \varepsilon_{it,a} + o_p\{(nI)^{-1/2}\}.$$

By Assumption 7, there exist coefficient vectors $\theta_{a,t}^* \in \mathbb{R}^M$ such that

$$\sup_{s \in \mathcal{S}} \left| \omega_t(a; \bar{A}_t, s) - \Psi(s)^\top \theta_{a,t}^* \right| = o\{(nI)^{-1/4}\}.$$

Therefore, uniformly in i and t ,

$$\omega_t(a; \bar{A}_{it}, S_{it}) \mathbb{I}\{A_{it} = a\} = \Psi(S_{it})^\top \theta_{a,t}^* \mathbb{I}\{A_{it} = a\} + o\{(nI)^{-1/4}\}.$$

By the exponential β -mixing property (Assumption 6) and bounded second moments, the contribution of this $o\{(nI)^{-1/4}\}$ approximation error vanishes after summation. In particular,

$$\frac{1}{nI} \sum_{i=1}^I \sum_{t=0}^{n-1} \left[\omega_t(a; \bar{A}_{it}, S_{it}) - \Psi(S_{it})^\top \theta_{a,t}^* \right] \mathbb{I}\{A_{it} = a\} \varepsilon_{it,a} = o_p\{(nI)^{-1/2}\}.$$

Consequently,

$$\frac{1}{nI} \sum_{i=1}^I \sum_{t=0}^{n-1} \omega_t(a; \bar{A}_{it}, S_{it}) \varepsilon_{it,a} = \frac{1}{nI} \sum_{i=1}^I \sum_{t=0}^{n-1} \Psi(S_{it})^\top \theta_{a,t}^* \mathbb{I}\{A_{it} = a\} \varepsilon_{it,a} + o_p\{(nI)^{-1/2}\}.$$

Next, by the projected Bellman moment condition onto the basis $\Psi(\cdot)$,

$$\int_{\mathcal{S}} \Psi(s) \mathbb{E} \left[\omega_t(a; \bar{A}_t, s) \mathbb{I}\{A_t = a\} \{\Psi(S_t) - \gamma \Psi(S_{t+1})\}^\top \right] G(ds) = \int_{\mathcal{S}} \Psi(s) G(ds).$$

Replacing $\omega_t(a; \bar{A}_t, s)$ by $\Psi(s)^\top \theta_{a,t}^*$ and using the $o\{(nI)^{-1/4}\}$ approximation error, we obtain

$$\Sigma_a(t) \theta_{a,t}^* = \int_{\mathcal{S}} \Psi(s) G(ds) + o\{(nI)^{-1/4}\},$$

where

$$\Sigma_a(t) := \frac{1}{nI} \sum_{i=1}^I \sum_{t=0}^{n-1} \mathbb{E} \left[\Psi(S_{it}) \mathbb{I}\{A_{it} = a\} \{\Psi(S_{it}) - \gamma \Psi(S_{i,t+1})\}^\top \right].$$

Hence

$$\theta_{a,t}^* = \Sigma_a(t)^{-1} \int_{\mathcal{S}} \Psi(s) G(ds) + o\{(nI)^{-1/4}\}.$$

Substituting this into the summation, we have

$$\begin{aligned} & \frac{1}{nI} \sum_{i=1}^I \sum_{t=0}^{n-1} \Psi(S_{it})^\top \theta_{a,t}^* \mathbb{I}\{A_{it} = a\} \varepsilon_{it,a} \\ &= \frac{1}{nI} \sum_{i=1}^I \sum_{t=0}^{n-1} \Psi(S_{it})^\top \left[\Sigma_a(t)^{-1} \int_{\mathcal{S}} \Psi(s) G(ds) \right] \mathbb{I}\{A_{it} = a\} \varepsilon_{it,a} + o_p((nI)^{-1/2}) \\ &= \frac{1}{nI} \sum_{i=1}^I \sum_{t=0}^{n-1} \left(\int_{\mathcal{S}} \Psi(s) G(ds) \right)^\top \Sigma_a(t)^{-1} \Psi(S_{it}) \mathbb{I}\{A_{it} = a\} \varepsilon_{it,a} + o_p((nI)^{-1/2}). \end{aligned}$$

Combining the above results, we obtain the first-order expansion

$$\hat{\tau} - \tau_0 = \frac{1}{nI} \sum_{i=1}^I \sum_{t=0}^{n-1} \left(\int_{\mathcal{S}} \Psi(s) G(ds) \right)^\top \Sigma_a(t)^{-1} \Psi(S_{it}) \mathbb{I}\{A_{it} = a\} \varepsilon_{it,a} + o_p((nI)^{-1/2}).$$

This completes Part 2.

Part 3 Define

$$Z_{it} := \left(\int_{\mathcal{S}} \Psi(s) G(ds) \right)^\top \Sigma_a(t)^{-1} \Psi(S_{it}) \mathbb{I}\{A_{it} = a\} \varepsilon_{it,a}.$$

From Part 2, we can write

$$\sqrt{nI} (\hat{\tau} - \tau_0) = \frac{1}{\sqrt{nI}} \sum_{i=1}^I \sum_{t=0}^{n-1} Z_{it} + o_p(1).$$

We will apply a martingale central limit theorem to the array $\{Z_{it}\}$. First, note that by construction and the MA+CMIA conditions, $\mathbb{E}[Z_{it} \mid \mathcal{F}_{i,t-1}] = 0$ for each i, t , where $\mathcal{F}_{i,t-1}$ is the σ -field generated by $\{(S_{i,s}, A_{i,s}, Y_{i,s}) : s < t\}$. Moreover, under the boundedness and moment conditions (Assumption 9), the conditional variance $\mathbb{E}[Z_{it}^2 \mid \mathcal{F}_{i,t-1}]$ is uniformly bounded. Thus, $\{Z_{it}\}$ forms a martingale-difference array satisfying the Lindeberg–Lyapunov conditions for asymptotic normality.

Let

$$\sigma^2 := \lim_{nI \rightarrow \infty} \frac{1}{nI} \sum_{i=1}^I \sum_{t=0}^{n-1} \mathbb{E}[Z_{it}^2].$$

By the ergodicity (mixing) and stationarity of the process, this limit exists and equals

$$\sigma^2 = \int_S \int_S \Psi(s)^\top G(ds) \Sigma_a^{-1} \Omega_a \Sigma_a^{-1} \Psi(s') G(ds'),$$

where Ω_a is the long-run covariance matrix of the process $\{\Psi(S_t) \mathbb{I}\{A_t = a\} \varepsilon_{t,a}\}$, and $\Sigma_a = \lim_{t \rightarrow \infty} \Sigma_a(t)$ (which is nonsingular by Assumption 9).

By the martingale central limit theorem (Hall and Heyde, 1980), we conclude that

$$\frac{1}{\sqrt{nI}} \sum_{i=1}^I \sum_{t=0}^{n-1} Z_{it} \xrightarrow{d} N(0, \sigma^2),$$

as $nI \rightarrow \infty$. Equivalently,

$$\sqrt{nI} (\hat{\tau} - \tau_0) \xrightarrow{d} N(0, \sigma^2).$$

Part 4 Combining the results of Parts 1–3, we have shown that $\hat{\tau}$ is asymptotically normal with variance σ^2 equal to the theoretical efficiency bound. It remains to construct a consistent

estimator for this asymptotic variance. Define

$$\hat{\sigma}^2 := \frac{1}{(nI)^2} \sum_{i=1}^I \sum_{t=0}^{n-1} \left[\left(\int_{\mathcal{S}} \Psi(s) G(ds) \right)^{\top} \hat{\Sigma}_a^{-1} \Psi(S_{it}) \mathbb{I}\{A_{it} = a\} \hat{\varepsilon}_{it,a} \right]^2,$$

where $\hat{\Sigma}_a$ and $\hat{\varepsilon}_{it,a}$ are consistent estimators of Σ_a and $\varepsilon_{it,a}$ based on the observed data. Under the regularity assumptions 6–9, standard uniform convergence and ergodicity arguments (see, e.g., the proof of Lemma 3 in Shi et al., 2022a) imply that $\hat{\sigma}^2 \xrightarrow{p} \sigma^2$. By Slutsky's lemma, it follows that

$$\frac{\sqrt{nI} (\hat{\tau} - \tau_0)}{\hat{\sigma}} \xrightarrow{d} N(0, 1).$$

This completes the proof of Theorem 2.